Proceedings of the 2000 IEEE/RSJ International Conference on Intelligent Robots and Systems

Analysis and Initial Experiments for a Novel Elephant's Trunk Robot

M.W. Hannan

Dept. Electrical/Computer Engineering
Clemson University
Clemson, SC 29634 USA
mhannan@ces.clemson.edu

I.D. Walker

Dept. Electrical/Computer Engineering
Clemson University
Clemson, SC 29634 USA
ianw@ces.clemson.edu

Abstract

The idea of studying tentacle and trunk type biological manipulation is not new, but there has been little progress in the development and application of physical devices to simulate these types of manipulation. Our research in this area is centered on a novel 'elephant trunk' robot. In this paper, we review the construction of the robot and how it compares to biological manipulators. We then apply our previously designed kinematic model to describe the kinematics of the robot. We finish by providing some examples of intelligent manipulation using the robot.

1 Introduction

As in nature, robot manipulators with a relatively small number of joints (i.e. arm type manipulators) are used for a large and diverse number of tasks. Though these types of manipulators are well understood and commonly used, they are best suited for obstacle free environments where the manipulator only interacts with the environment using its end-effector. Compare this with the abilities of a variety of creatures in the natural world. Animals such as squid, elephants, and snakes exhibit a wide array of successful locomotions and behaviors [6]. The abilities of these biological manipulators present an interesting and challenging topic for robotics.

The maneuverability inherent in the above types of biological structures allows them to negotiate obstacle fields of significant complexity compared to conventional robots. These structures also have the ability to conform to environmental constraints on contact. This compliance can be extremely useful in a wide range of situations, such as using the manipulator's entire structure for 'whole-arm' manipulation. Therefore these types of structures have significant potential for improved performance over traditional manipulators in the areas of obstacle avoidance and manipulation.

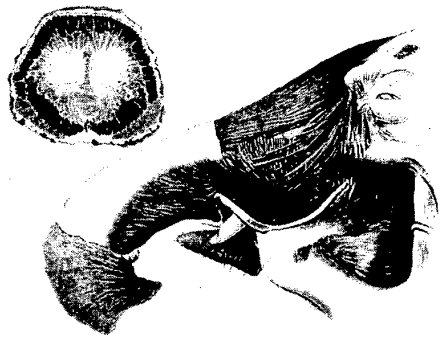

Figure 1: Muscle Structure of an Elephant

Notice that the examples of tentacles and trunks in the preceding discussion are invertebrate type structures. Snakes are vertebrates, but possess such a large number of joints in their backbone that they can exhibit the functionality and properties of invertebrate creatures. These types of backbone structures have been termed 'hyper-redundant' in the robotics community [1]. These robots feature a dramatic excess of joints, and hence can assume a wide range of shapes and configurations. There has been significant interest in, and analysis of these types of devices over the last few years. However, most of the work in this area has been in analyzing the kinematics, and not in the physical implementation of these types of manipulators.

0-7803-6348-5/00/$10.00 ©2000 IEEE.

2 Design Considerations

Biological trunks and tentacles are constructed almost entirely of muscle, and have no skeletal structure for support [6], see Fig. 1. The arrangement of muscles not only provide the necessary forces for movement, but also has the property of supplying the needed forces for structural support. The main stumbling block in building a useful mechanical equivalent of these biological manipulators is the need to simulate muscles. Presently, there are no actuators that can compare in both size and performance of that obtainable by biological muscles. Therefore, present actuator technology must be used to try to reproduce the same effects as the muscles do in trunk and tentacle type manipulators.

Before an actuation strategy can be devised, there are two main properties in trunk/tentacle manipulators that must be addressed. The first is that of structural support. The idea is to design a structure that has an inherent 'bending stiffness.' In biological manipulators this bending stiffness is generated by the contraction of muscles. The amount of stiffness is the physical property that will determine the overall shape of the manipulator. *This is very important in that without sufficient bending stiffness, the manipulator will sag under its own weight, or buckle when used for manipulation.* The second important design consideration is that of movement. The actuation strategy can theoretically incorporate three different movements: bending, elongation, and twisting. A manipulator does not have to exhibit all three properties, and actuation for pure bending is most often desired.

The previous design considerations can be reached in many different ways [9], but the use of a cable/tendon actuation system has been most often used in the relatively few attempts at hardware implementations, [2] [4] [5] [14]. In the basic arrangement, the manipulator is constructed with some type of 'backbone' structure. The backbone can either be segmented (interconnected with joints) or it can be a continuous structure. In the case of a continuous backbone structure, the backbone usually performs two functions. It provides the overall form for the manipulator, and it also can supply the needed 'bending stiffness' through its physical properties, [2] [4]. A segmented backbone can provide the form of the manipulator, but requires some type of external device to supply the bending stiffness (i.e. springs). Alternatively, the backbone can be replaced with a fluid filled bellow [5]. The shape of these manipulators is then controlled through the use of antagonistic sets of cables, where cables are changed in length to actuate the manipulator. If the cables have different relative lengths they can invoke a bend in the manipulator. If the backbone can change length, then an equal change in the cable lengths can cause elongation in the manipulator.

Another possible approach is to use fluids for actuation [12]. The manipulator can be composed of several elastic, fluid filled tubes that are radially mounted around the center line of the manipulator. The motion of the manipulator is obtain by changing the relative pressures in the tubes. This change in relative pressure between the tubes will cause the manipulator to bend or elongate.

3 Elephant Trunk Manipulator's Construction

Figure 2: 'Elephant Trunk' Manipulator

The construction of our 'elephant trunk' manipulator [14] resembles that of a spinal column, see Fig. 2, with a total length of 83.82 cm. It is composed of a total of 16 two degree of freedom joints yielding a total of 32 degrees of freedom (DOF) for the backbone. The manipulator is then divided into four main sections ranging in diameter from 10.16 cm, 8.89 cm, 7.62 cm, and down to 6.35 cm for the end section. Each of the four sections is composed of four joints. The actuation of these sections is provided through the use of a hybrid cable and spring servo system. Located between each pair of joints is a cylindrical shaped segment that acts as a conduit for routing the cables, and as the anchor for each set of springs. The series combination of the segments gives the manipulator its defining shape, and every fourth segment serves as an anchor for each set of cables.

The overall motion of the manipulator is controlled by a tendon (cable) servo system, see Fig. 3. The cables are actuated remotely by d.c. motors via a pulley system that is fitted with with cable tensioning devices. The cables are arranged into sets of antagonistic pairs. Each set actuates one of the two DOF per section. There is a second set of cables that is rotated 90 degrees from the first set, and is used to

Figure 3: Cable Actuation System

actuate the second DOF. The actuation is produced by one of the cables in a set exerting a force on the anchoring segment, which in turn generates a moment at that joint. As this joint rotates, it causes adjacent segments to move closer or farther apart, which then causes the springs to compress or extend. Thus, the springs, which are anchored at some distance normal to the joint, exert a force between the adjacent segments providing a transfer of torque to the adjacent joints. This interconnection of the joints, links, and springs is what gives the manipulator its curved appearance, and yields a total of eight independently actuated DOF [14].

Due to the large number of joints and the inability to mount measurement devices for the joint angles, determining the shape of the manipulator is not simple. There are a few possibilities that allow a direct measurement of the shape of the manipulator, i.e. image processing and fiber optics ($SHAPE\,TAPE^{TM}$, Measurand Inc.), but are usually very difficult and costly to implement on a three dimensional robot. Another plausible solution is to use the geometry of the manipulator, the change in cable lengths, and the assumption that each joint in a section rotates by the same amount. An approximate curvature can then be fitted to each section of the manipulator [3]. A formula for calculating the joint angle in one section, on the side of the manipulator where the cable length is decreasing, is

$$\theta = \pi - 2\arctan\left(\frac{w}{h}\right) - \arctan\left(\frac{\sqrt{4r^4 - \left\{2r^2 - (l-\Delta l)^2\right\}^2}}{2r^2 - (l-\Delta l)^2}\right), \quad (1)$$

where w is the radius of a segment, h is the distance from the center of a segment to the center of the joint, $r = \sqrt{w^2 + h^2}$, l is the original cable length, and Δl is the change in cable length. From [3],

$$k = \frac{2\phi}{s}, \quad (2)$$

where k is the curvature of a section, s is the total arc length of a section, and ϕ is the angle of the position vector to the end of one section. From the kinematics of a four section robot, it can be determined that

$$\phi = 2\theta. \quad (3)$$

Therefore, we can determine an approximate curvature for a section given the changes in cable length from Eq. (1), (2), and (3). Note, this is an approximation for the curvature. Due to the fact that the section has a jointed backbone and not a continuous backbone, s is not constant. However, the change in s is small and can be approximated to be constant.

4 Motion Planning

Due to the continuous nature of these tentacle and trunk type manipulators, using joint angles and link lengths does not supply an easy and physically realizable description of the manipulator's shape. If instead the kinematic model uses curvatures to describe the shape, the model provides a more physically and intuitive description of the manipulator. In [3], we used constant curvature sections to describe the kinematics of these types of manipulators. If each section is designed so that it bends with constant curvature [7], we can use differential geometry and some standard robotic techniques to generate a kinematic model. The kinematic model can be applied in either the planar or spatial case, but for simplicity and conciseness we will apply the model to the planar case here (moving the elephant's trunk robot in a plane).

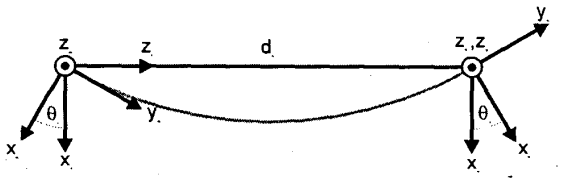

Figure 4: Denavit-Hartenberg Frames for a Planar Section

From [3], the movement of a planar curve with constant curvature, κ, and fixed arc length, s, can be described by three coupled movements:

1. rotation by an angle θ
2. translation by an amount of $\|\mathbf{x}\|$
3. rotation by the angle θ again

where $\mathbf{x}$ is the position vector of the end-point,

$$\theta = \frac{\kappa\, s}{2}, \tag{4}$$

and

$$\|\mathbf{x}\| = \frac{s}{\theta}\sin(\theta). \tag{5}$$

Note that Eq. (5) is a function of the angle θ, therefore there is a coupling between the magnitude and 'phase' angle of $\mathbf{x}$. If the Denavit-Hartenberg (D-H) frames for one section are setup as in Fig. 4, then the D-H table is

link	θ	d	a	α
1	*	0	0	-90°
2	0	*	0	90°
3	*	0	0	0°

Using the D-H table, the homogeneous transformation matrix for one section, i.e. from frame 0 to frame 3, in terms of the curvature κ and the total arc length l of the curve as

$$A_0^3 = \begin{bmatrix} \cos(\kappa l) & -\sin(\kappa l) & 0 & \frac{1}{\kappa}\{\cos(\kappa l) - 1\} \\ \sin(\kappa l) & \cos(\kappa l) & 0 & \frac{1}{\kappa}\sin(\kappa l) \\ 0 & 0 & 1 & 0 \\ 0 & 0 & 0 & 1 \end{bmatrix}. \tag{6}$$

The parameter l is used to give the position of the end point of the section. **Note**, if the point of interest lies some where between 0 and l, then the corresponding value of arc length can be used instead.

The same technique can be used for the spatial case [3], where the frames are given in figure 5 and the D-H table is

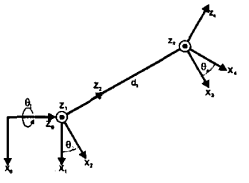

Figure 5: Denavit-Hartenberg Frames for a 3-D Section

link	θ	d	a	α
1	*	0	0	90°
2	*	0	0	-90°
3	0	*	0	90°
4	*	0	0	-90°

The kinematics for a four section continuum robot can be setup as a combination of four sections. Using the simple and repetitive structure of the D-H table, the transformation matrix used for the forward kinematics is the product of four matrices of the form of Eq. (6). Therefore, the transformation matrix from frame 0 to frame 12 is

$$A_0^{12} = \begin{bmatrix} A_{11} & A_{12} & 0 & A_{14} \\ A_{21} & A_{22} & 0 & A_{24} \\ 0 & 0 & 1 & 0 \\ 0 & 0 & 0 & 1 \end{bmatrix}. \tag{7}$$

The previously undefined matrix elements are given in appendix A, where κ_i and l_i are the curvature and total arc length respectively for *section* i and $\omega_i = \kappa_i l_i$ for $i = \{1,2,3,4\}$. **Note**, the total arc length for $i = \{1,2,3\}$ must be used so that *section 4* is properly oriented, but any arc length can be used for the final section depending on where the point of interest lies in the section. The total arc length for the final section gives the kinematics in terms of the end point of the final section.

The velocity kinematics can be written as

$$\dot{\mathbf{x}} = J\dot{\mathbf{q}}, \tag{8}$$

where $\dot{\mathbf{x}} = \begin{bmatrix} \dot{x} & \dot{y} \end{bmatrix}^T$ and $\dot{\mathbf{q}} = \begin{bmatrix} \dot{\kappa}_1 & \dot{\kappa}_2 & \dot{\kappa}_3 & \dot{\kappa}_4 \end{bmatrix}^T$. Note that in contrast to that for the traditional manipulator Jacobian, the relationship here is between manipulator *curvatures* and task variables. In essence, curvatures replace the joint angles here. The Jacobian, J, is as follows:

$$J = \begin{bmatrix} J_{11} & J_{12} & J_{13} & J_{14} \\ J_{21} & J_{22} & J_{23} & J_{24} \end{bmatrix}, \tag{9}$$

where the elements of J are given in appendix B. Using the minimum norm solution for the inverse of J, $J^+ = J^T\left(JJ^T\right)^{-1}$, the curvatures needed for a desired end-point position can be determined using Eq. (8). Now that we have the velocity kinematics, the manipulator can be controlled using redundancy techniques [8] [10] [13].

One useful and effective technique is that of task decomposition [13]. The concept is to perform the highest priority subtask first. If there is any redundancy not used for the first subtask, then the 'left over' redundancy is used to complete a second subtask and so on. This can easily be applied to manipulation as follows. The general solution is given as

$$\dot{\mathbf{q}} = J^+\dot{\mathbf{x}} + \left(I - J^{-1}J\right)\mathbf{q}_0, \tag{10}$$

where $\mathbf{q}_0 \in R^m$. The term $J^+\dot{\mathbf{x}}$ in Eq. (10) is the minimum norm solution, and $\left(I - J^{-1}J\right)\mathbf{q}_0$ is the null

space solution [13]. A simple manipulation strategy is to specify the desired constant configuration needed for manipulation (grasping) of an object. The first subtask is used to move the end-point of the manipulator on a desired trajectory $\mathbf{x}_d(t) \in R^n$, and the second subtask is used to obtain the desired constant configuration $\mathbf{q}_d \in R^m$ needed for manipulation. From [13], the control law for such a task is given as

$$\begin{aligned} \dot{\mathbf{q}} = \quad & J^+ \{\dot{\mathbf{x}}_d - H_1 (\mathbf{x} - \mathbf{x}_d)\} \\ & - (I - J^+ J) H_2 (\mathbf{q} - \mathbf{q}_d) k, \end{aligned} \tag{11}$$

where $H_1 \in R^{n \times n}$ and $H_2 \in R^{m \times m}$ are positive definite symmetric gain matrices and k is a positive constant.

5 Experimental Examples

Using the theory outlined in the previous sections, we have performed several experiments to show the use and flexibility of tentacle/trunk type manipulators.

Our first example is a planar manipulator following a desired linear trajectory for the end-point. The different configurations were generated using Eq. (9) and (10) with $\mathbf{q}_0 = 0$. In appendix C, figures 7 through 12 show a comparison between the simulated configurations at several points in the linear trajectory, and the corresponding photographic snapshots of the physical robot at the same points. Snapshots of the manipulator are shown due to the lack of ability to precisely measure the robots end-point location, therefore the error $\mathbf{x}_d - \mathbf{x}$ can not be verified in a practical fashion. It is important to understand that manipulators of this design are *not well suited to high precision applications* due to their actuation and physical construction, but are instead *best suited for applications where their flexibility and compliance can be exploited.*

The second example is the manipulation of a circular object. The robot is given a desired configuration needed to grasp the object, $\mathbf{q}_d$, then Eq. (10) is used to approach the object and obtain the desired configuration. The robot then uses Eq. (10) to move the object around. Figure 6 shows a snapshot of the robot executing the manipulaton task, only one picture is given for compactness of the paper.

6 Conclusions

We have discussed the design, construction, and operation of a novel 'elephant's trunk' robot and how it compares to biological manipulators. The potential of this type of manipulator for enhanced manipulation is noted, and special issues and problems associated with construction and analysis of this class of robots was discussed. We discuss the application of our previously designed kinematic model to describe the (positional and differential motion) kinematics of the robot. It is shown how established resolved-rate and redundancy resolution schemes can be utilized for motion planning for the device, using local curvatures as substitutes for traditional joint variables. Examples of intelligent manipulation using the robot were also given.

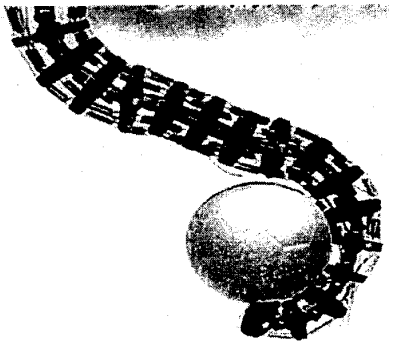

Figure 6: Manipulation of Circular Object

References

[1] G.S. Chirikjian, "Theory and Applications of Hyper-Redundant Robotic Mechanisms," *Ph.D. Thesis Dept. of Applied Mechanics*, California Institute of Technology, 1992.

[2] R. Cieslak, A. Morecki, "Elephant Trunk Type Elastic Manipulator - A Tool for Bulk and Liquid Materials Transportation" *Robotica*, Vol. 17, pp. 11-16, 1999.

[3] M.W.Hannan, I.D. Walker, "Novel Kinematics for Continuum Robots," *7th International Symposium on Advances in Robot Kinematics, Slovenia*, pp. 227-238, 2000.

[4] S. Hirose, *Biologically Inspired Robots*, Oxford University Press, 1993.

[5] G. Immega, K. Antonelli, "The KSI Tentacle Manipulator," *IEEE Conf. on Robotics and Automation*, pp. 3149-3154, 1995.

[6] W.M. Kier, K.K. Smith, "Tongues, Tentacles, and Trunks: The Biomechanics of Movement in Muscular hydrostats," *Zoological Journal of the Linnean Society*, Vol. 83, pp. 307-324,1985.

[7] C. Li, C.D. Rahn, "Nonlinear Kinematics for a Continuous Backbone, Cable-Driven Robot," *To Appear at the 20th Southeastern Conf. on Theoretical and Applied Mechanics*, 2000.

[8] D.N. Nenchev, "Redundancy Resolution through Local Optimization: A Review," *Journal of Robotic Systems*, vol. 6, pp. 769-798, 1989.

[9] G. Robinson, J.B.C. Davies, "Continuum Robots - A State of the Art," *IEEE Int. Conf. on Robotics and Automation*, pp. 2849-2854, 1999.

[10] B. Siciliano, "Kinematic Control of Redundant Robot Manipulators: A Tutorial," *Journal of Intelligent and Robotic Systems*, Vol. 3, pp. 201-212, 1990.

[11] K.K. Smith, W.M. Kier, "Trunks, Tongues, and Tentacles: Moving with Skeletons of Muscle," *American Scientist*, Vol. 77, pp. 28-35, 1989.

[12] K. Suzumori, S. Iikura, H. Tanaka, "Development of Flexible Microactuator and its Applications to Robotic Mechanisms," *IEEE Int. Conf. on Robotics and Automation*, pp. 1622-1627, 1991.

[13] T. Yoshikawa, "Analysis and Control of Robot Manipulators with Redundancy,", in *Robotics Research - The First International Symposium*, Brady and Paul, eds., MIT Press, Cambridge, MA, pp. 735-747, 1985.

[14] I.D. Walker, M.W. Hannan "A Novel Elephant's Trunk Robot," *IEEE/ASME Int. Conf. on Advanced Intelligent Mechatronics*, pp. 410-415, 1999.

Appendix A

$$A_{11} = \cos(\omega_1+\omega_2+\omega_3+\omega_4)$$

$$A_{21} = \sin(\omega_1+\omega_2+\omega_3+\omega_4)$$

$$A_{12} = -\sin(\omega_1+\omega_2+\omega_3+\omega_4)$$

$$A_{22} = \cos(\omega_1+\omega_2+\omega_3+\omega_4)$$

$$A_{14} = \frac{\cos\omega_1-1}{\kappa_1} + \frac{\cos(\omega_1+\omega_2)-\cos\omega_1}{\kappa_2} + \frac{\cos(\omega_1+\omega_2+\omega_3)-\cos(\omega_1+\omega_2)}{\kappa_3} + \frac{\cos(\omega_1+\omega_2+\omega_3+\omega_4)-\cos(\omega_1+\omega_2+\omega_3)}{\kappa_4}$$

$$A_{24} = \frac{\sin\omega_1}{\kappa_1} + \frac{\sin(\omega_1+\omega_2)-\sin\omega_1}{\kappa_2} + \frac{\sin(\omega_1+\omega_2+\omega_3)-\sin(\omega_1+\omega_2)}{\kappa_3} + \frac{\sin(\omega_1+\omega_2+\omega_3+\omega_4)-\sin(\omega_1+\omega_2+\omega_3)}{\kappa_4}$$

Appendix B

$$J_{11} = \frac{-l_1\sin\omega_1}{k_1} + \frac{l_1\{-\sin(\omega_1+\omega_2)+\sin\omega_1\}}{k_2} + \frac{l_1\{-\sin(\omega_1+\omega_2+\omega_3)+\sin(\omega_1+\omega_2)\}}{k_3} + \frac{l_1\{-\sin(\omega_1+\omega_2+\omega_3+\omega_4)+\sin(\omega_1+\omega_2+\omega_3)\}}{k_4} - \frac{\cos\omega_1-1}{k_1^2}$$

$$J_{12} = -\frac{\cos(\omega_1+\omega_2)-\cos\omega_1}{k_2^2} - \frac{l_2\sin(\omega_1+\omega_2)}{k_2} + \frac{l_2\{-\sin(\omega_1+\omega_2+\omega_3)+\sin(\omega_1+\omega_2)\}}{k_3} + \frac{l_2\{-\sin(\omega_1+\omega_2+\omega_3+\omega_4)+\sin(\omega_1+\omega_2+\omega_3)\}}{k_4}$$

$$J_{13} = -\frac{l_3\sin(\omega_1+\omega_2+\omega_3)}{k_3} + \frac{l_3\{-\sin(\omega_1+\omega_2+\omega_3+\omega_4)+\sin(\omega_1+\omega_2+\omega_3)\}}{k_4} - \frac{\cos(\omega_1+\omega_2+\omega_3)-\cos(\omega_1+\omega_2)}{k_3^2}$$

$$J_{14} = -\frac{l_4\sin(\omega_1+\omega_2+\omega_3+\omega_4)}{k_4} - \frac{\cos(\omega_1+\omega_2+\omega_3+\omega_4)-\cos(\omega_1+\omega_2+\omega_3)}{k_4^2}$$

$$J_{21} = -\frac{\sin\omega_1}{k_1^2} - \frac{l_1\cos\omega_1}{k_1} + \frac{l_1\{\cos(\omega_1+\omega_2)-\cos\omega_1\}}{k_2} + \frac{l_1\{\cos(\omega_1+\omega_2+\omega_3)-\cos(\omega_1+\omega_2)\}}{k_3} + \frac{l_1\{\cos(\omega_1+\omega_2+\omega_3+\omega_4)-\cos(\omega_1+\omega_2+\omega_3)\}}{k_4}$$

$$J_{22} = -\frac{\sin(\omega_1+\omega_2)-\sin\omega_1}{k_2^2} + \frac{l_2\cos(\omega_1+\omega_2)}{k_2} + \frac{l_2\{\cos(\omega_1+\omega_2+\omega_3)-\cos(\omega_1+\omega_2)\}}{k_3} + \frac{l_2\{\cos(\omega_1+\omega_2+\omega_3+\omega_4)-\cos(\omega_1+\omega_2+\omega_3)\}}{k_4}$$

$$J_{23} = \frac{l_3\cos(\omega_1+\omega_2+\omega_3)}{k_3} + \frac{l_3\{\cos(\omega_1+\omega_2+\omega_3+\omega_4)-\cos(\omega_1+\omega_2+\omega_3)\}}{k_4} - \frac{\sin(\omega_1+\omega_2+\omega_3)-\sin(\omega_1+\omega_2)}{k_3^2}$$

$$J_{24} = \frac{l_4\cos(\omega_1+\omega_2+\omega_3+\omega_4)}{k_4} - \frac{\sin(\omega_1+\omega_2+\omega_3+\omega_4)-\sin(\omega_1+\omega_2+\omega_3)}{k_4^2}$$

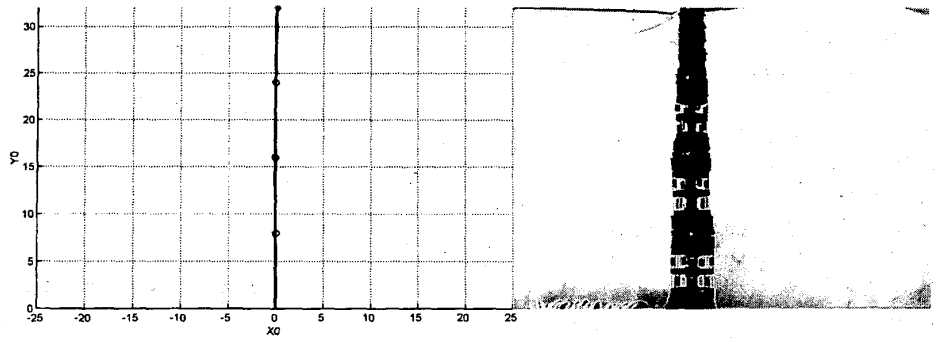

Figure 7: Linear Trajectory - Snapshot 1

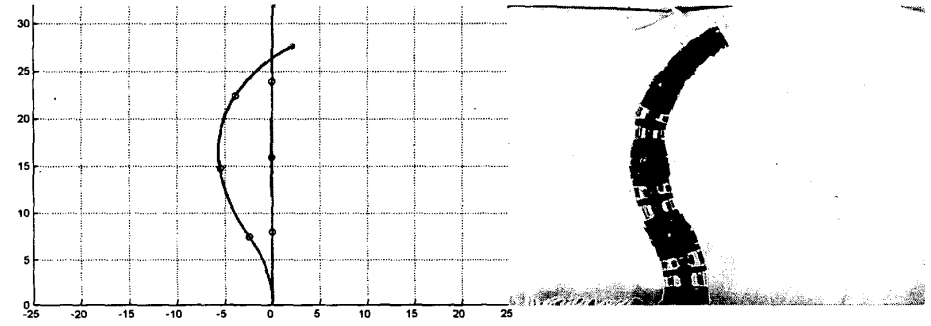

Figure 8: Linear Trajectory - Snapshot 2

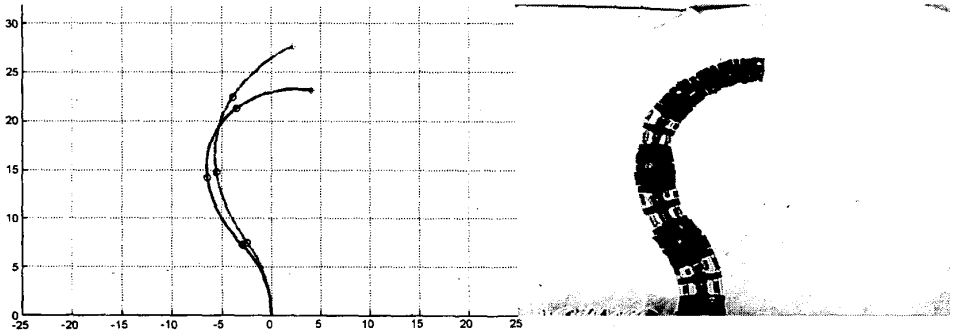

Figure 9: Linear Trajectory - Snapshot 3

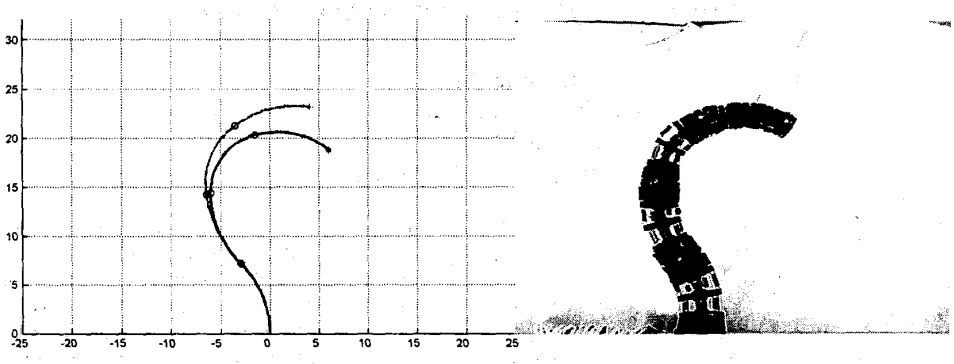

Figure 10: Linear Trajectory - Snapshot 4

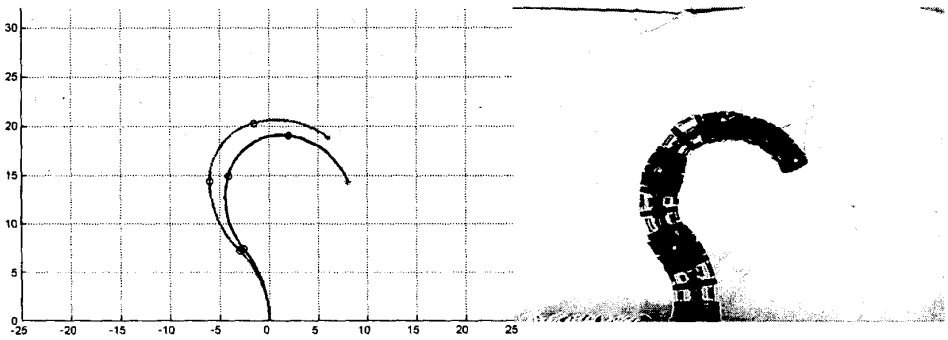

Figure 11: Linear Trajectory - Snapshot 5

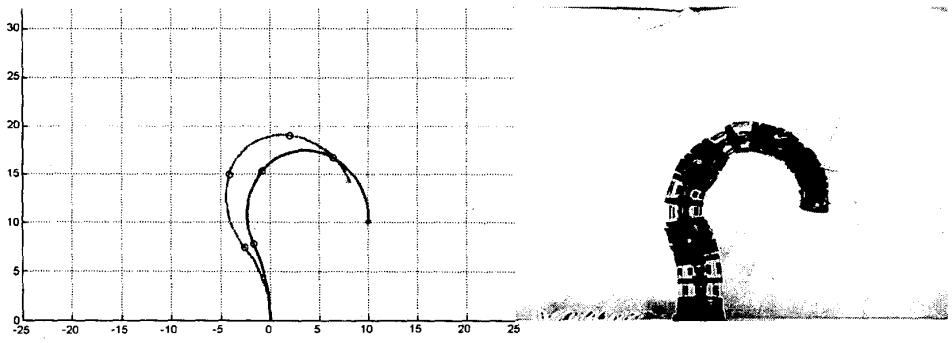

Figure 12: Linear Trajectory - Snapshot 6